Available online at www.sciencedirect.com
ScienceDirect
Journal of Organometallic Chemistry 692 (2007) 4774–4783
Journal of Organometallic Chemistry
www.elsevier.com/locate/jorganchem

Heterolytic CH-bond activation in the synthesis of Ni{(2-aryl-κC^2)pyridine-κN}$_2$ and derivatives

Emily C. Volpe, Andrew R. Chadeayne, Peter T. Wolczanski *, Emil B. Lobkovsky

Department of Chemistry and Chemical Biology, Baker Laboratory, Cornell University, Ithaca, NY 14853, United States

Received 3 May 2007; received in revised form 5 June 2007; accepted 7 June 2007
Available online 30 June 2007

Dedicated to Prof. Gerhard Erker on the occasion of his 60[th] birthday; Zirconium, it's in our blood.

Abstract

Thermolysis of Ni(OTf)$_2$ in 2-phenyl-pyridine or 2-tolyl-pyridine afforded the cationic chelate derivatives, [bis(2-aryl-pyridine)Ni{(2-aryl-κC^2)pyridine-κN}]OTf (aryl = phenyl, **1a**; tolyl, **1b**). Addition of KBr to **1a** and LiBr to **1b** provided the bromides, (2-aryl-pyridine)BrNi{(2-aryl-κC^2)pyridine-κN} (aryl = phenyl, **2a**; tolyl, **2b**). When subjected to KO^{t}Bu in Et$_2$O, the bromides generated the entitled bis-cyclometalated compounds, Ni{(2-aryl-κC^2)pyridine-κN}$_2$ (aryl = phenyl, **3a**; tolyl, **3b**). These compounds insert diphenylacetylene into one cyclometalate arm to produce [(2-aryl-κC^2)pyridine-κN]Ni[2-(2-(1,2-diphenylethenyl-κC^2)aryl)pyridine-κN] (aryl = phenyl, **4a**; *p*-tolyl, **4b**). X-ray crystallographic studies were conducted on **1a**, **2a**, **3a** and **4a**, and a brief DFT study of **3a** confirmed its low spin configuration and rippled geometry.

Keywords: Nickel; CH-bond activation; Alkyne; Insertion; Triflate; Cyclometalation

1. Introduction

In order to impart stronger ligand fields on 1st-row transition metals, the use of metal–carbon bonds, especially metal–aryl bonds, remains an intriguing possibility [1]. In angular overlap parlance, the ΔE_{MAr} for such bonds – the energy match between metal and C-based orbitals – is small when compared to more electronegative second row main group elements (e.g., O, N), and the orbital overlap is also significant in comparison [2]. The critical problem that must be overcome is the intrinsic reactivity of the metal–aryl bond.

Metal–aryl bonds can be entrained within chelates to add kinetic stability, and heterolytic CH-bond activation was considered as an efficient means to synthesize complexes containing such ligands [3–5]. There are various approaches to the synthesis of metal–carbon bonds, the most common being metathesis and oxidative addition (OA) [6,7]. Since either of these requires a functionalization (ArX/M′) of the aryl group (i.e., X = halogen; M′ = Li, MgX), CH-bond activation eliminates these steps. In principle, an electrophilic metal center MX_n can react with a chelate L-ArH to produce (L-Ar)MX_{n-1} and HX, where X is likely to be halide, OTf, O_2CCF_3, etc. Transition metal triflates are an attractive class of starting materials for an exploratory study of this type, and 2-phenyl-pyridine has considerable precedent in heterolytic CH-bond activations [8–18]. The use of Ni(OTf)$_2$ [19] as a starting material capable of heterolytically activating 2-phenyl-pyridine, and subsequent reactivity studies are reported herein.

2. Results

2.1. Heterolytic 2-phenyl-pyridine activation by Ni(OTf)$_2$

2.1.1. Synthesis of [bis(2-aryl-pyridine)Ni{(2-aryl-κC^2)pyridine-κN}]OTf

As Scheme 1 illustrates, thermolysis of Ni(OTf)$_2$ in neat 2-phenyl-pyridine or 2-tolyl-pyridine afforded the cationic

* Corresponding author.
E-mail address: ptw2@cornell.edu (P.T. Wolczanski).

0022-328X/$ - see front matter © 2007 Elsevier B.V. All rights reserved.
doi:10.1016/j.jorganchem.2007.06.047

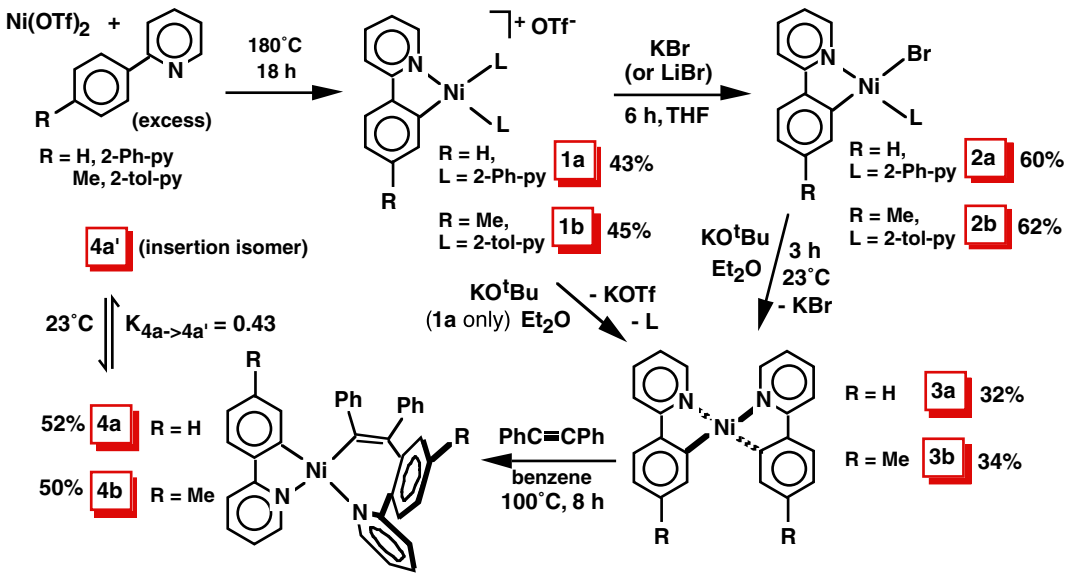

Scheme 1.

chelate derivatives, [bis(2-aryl-pyridine)Ni{(2-aryl-κC^2)pyridine-κN}]OTf (aryl = phenyl, **1a**; tolyl, **1b**), in modest yield (~40–45%). ^{1}H NMR spectroscopy on these sparingly soluble yellow compounds revealed two η^1-N-bound 2-aryl-pyridines, and a related group lacking an *ortho*-H on an asymmetric phenyl residue, suggesting that heterolytic CH-bond activation had indeed occurred. ^{1}H NMR spectra for all new compounds can be found in Table 1, and ^{13}C{^{1}H} NMR spectra for those compounds soluble enough for ready characterization are found in Table 2.

Table 1
^{1}H NMR data (δ, *J* (Hz); benzene-d_6) for [bis(2-aryl-pyridine)Ni{(2-aryl-κC^2)pyridine-κN}]OTf (aryl = phenyl, **1a**; tolyl, **1b**), [(2-aryl-pyridine)BrNi{(2-aryl-κC^2)pyridine-κN}] (aryl = phenyl, **2a**; tolyl, **2b**), Ni{(2-aryl-κC^2)pyridine-κN}$_2$ (aryl = phenyl, **3a**; tolyl, **3b**), and [(2-aryl-κC^2)pyridine-κN]Ni[2-(2-(1,2-diphenylethenyl-κC^2)aryl)pyridine-κN] (aryl = phenyl, **4a**; tolyl, **4b**)[a]

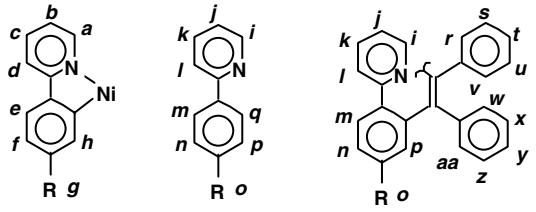

	ab (*i*)	*c* (*j*)	*d* (*k*)	*e* (*l*)	*f* (*m*)	*g* (*n*)	*h* (*o*)	*q* (*p*)	(*r*–*aa*)
1a	9.29(5.5)	6.08	6.46(8.5)	6.52	8.40(6.0)	7.12	7.12	5.49(8.0)	7.99(7.5)
	8.56(8.5)	6.87–6.76	6.64–6.58	6.76–6.87	7.99(7.5)	7.21–7.20	7.03	7.21–7.20	
1b	9.36(5.5)	6.06	6.47	6.66(8.0)	8.43(6.0)	6.73(8.0)	2.09	5.41	8.00
	8.60(8.5)	7.02	6.52–6.58	6.87	8.00	7.00	1.89,1.91	7.08	
2a	9.94(7.0)	6.12(8.0)	6.56–6.63	6.83(5.0)	6.68–6.77	6.56–6.63	6.83	5.36(9.5)	8.90(9.0)
	9.45(6.5)	6.30(8.0)	6.97(9.5)	7.19	8.90(9.0)	6.68–6.77	7.19	6.68–6.77	
2b	9.54(5.5)	6.12(6.5)	6.60	6.67(8.0)	6.72–6.81	6.60	1.84	5.23	8.93(8.1)
	9.98(6.0)	6.33(6.5)	6.72–6.81	6.86(8.0)	8.93(8.0)	7.03(7.5)	1.98	7.03	
3a	7.72(5.0)	6.27(6.5)	6.92(7, 8)	7.12(8.5)	7.31(7.5)	7.35(7.0)	7.15	8.39(7.5)	
	7.73(5.6)	6.26(8.0)	6.94(10.0)	7.01(8.4)	7.33(8.0)	7.36(8.0)	2.35	8.22	
4a	7.79(5.5)	6.28(7.0)	6.77(7.5)	7.22	7.43(7.5)	7.30	7.30	7.49(8.0)	6.86–7.01
	7.06(7.5)	6.04(6.0)	6.85	7.22	7.30	7.11(7.5)	7.30	8.47(7.5)	
4b	7.84(4.0)	6.28(5.0)	6.78	7.18	7.40(7.5)	7.34(7.5)	2.49	7.44	6.87–7.06
	7.11(7.5)	6.04(5.0)	6.78	7.18	7.40(7.5)	7.34(7.5)	1.78	8.31	

[a] Shift assignments are based on correlations with free ligands, literature precedent and the accompanying compounds; the assignments are *tentative*. Coupling constants, where quoted, are phenomenological. First row corresponds to {(2-aryl-κC^2)pyridine-κN} ligand as shown in illustration; second row corresponds to remaining 2-aryl-pyridine or pyridine-derived fragment.

2.1.2. Structure of [bis(2-phenyl-pyridine)Ni{(2-phenyl-κC^2)pyridine-κN}]OTf

Table 3 lists crystallographic information pertaining to the structure of [bis(2-phenyl-pyridine)Ni{(2-phenyl-κC^2)pyridine-κN}]OTf (**1a**), and Fig. 1 provides a molecular view of the square planar cation. Unfortunately, while the structure confirms the cyclometalated (2-phenyl-κC^2)pyridine-κN unit, there is a 1:1 disorder in the pyridine and activated phenyl groups, thereby rendering virtually all metric parameters an average of the two orientations. As expected, the two 2-phenyl-pyridine ligands are oriented in the more sterically favorable "up and down" orientation with respect to the $(N_{py})_2Ni(\kappa C, \kappa N)$ plane, giving the molecule a crystallographic pseudo-2-fold axis bisecting the N_{py}–Ni–N_{py} angle.

2.1.3. Substitution by bromide

Displacement of the 2-aryl-pyridine ligands from [bis(2-aryl-pyridine)Ni{(2-aryl-κC^2)pyridine-κN}]OTf (aryl = phenyl, **1a**; tolyl, **1b**) proved to be difficult. The low volatility of 2-phenyl-pyridine prevented its ready removal after displacement, and the orientation of the bound 2-phenyl-pyridines hampers associative substitution processes expected for square planar Ni(II) by blocking sites above and below the plane. Persistent difficulties in substitution with neutral L′ prompted a switch to anionic nucleophiles in an effort to generate neutral Ni(II) species. Various R^- equivalents (MeLi, ^{t}BuCH$_2$Li, MeMgBr, etc.) generated red solutions from which no tractable material could be isolated. Success was achieved through the addition of KBr to **1a** and LiBr to **1b** to afford the bromides, (2-aryl-pyridine)BrNi{(2-aryl-κC^2)-pyridine-κN} (aryl = phenyl, **2a**; tolyl, **2b**). The compounds were again characterized by one complete 2-aryl-pyridine fragment and one lacking an *ortho*-H on the aryl, as Tables 1 and 2 reveal. The conformation of **2a**, as confirmed by a single crystal X-ray structure determination, is square planar, with the Br^- opposite the Ni–aryl bond. This geometry conforms to expectations based on the stronger *trans*-effect of the Ni–aryl bond in comparison to the pyridine–Ni bond of the chelate. In addition, no noticeable isomerization was observed under a variety of solvents (THF, toluene, benzene, CH_3CN) and conditions. In the *trans*-influence series, the

Table 2
$^{13}C\{^1H\}$ NMR data (benzene-d_6) for [bis(2-phenyl-pyridine)Ni{(2-phenyl-κC^2)pyridine-κN}]OTf (**1a**), [(2-aryl-pyridine)BrNi{(2-aryl-κC^2)pyridine-κN}] (aryl = phenyl, **2a**; tolyl, **2b**), Ni{(2-aryl-κC^2)pyridine-κN}$_2$ (aryl = phenyl, **3a**; tolyl, **3b**), and [(2-aryl-κC^2)pyridine-κN]Ni[2-(2-(1,2-diphenylethenyl-κC^2)aryl)pyridine-κN] (aryl = phenyl, **4a**; tolyl, **4b**)[a,b]

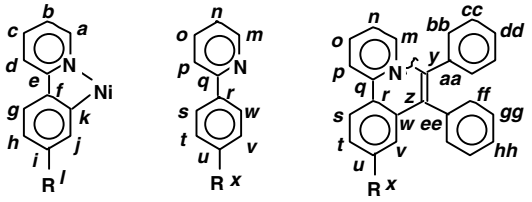

	a *m* *y*	*b* *n* *z*	*c* *o* *aa*	*d* *p* *bb*	*e* *q* *cc*	*f* *r* *dd*	*g* *s* *ee*	*h* *t* *ff*	*i* *u* *gg*	*j* *v* *hh*	*k* *w* *ii*	*l* *x*
1a	153.4 139.0 150.7	117.5 122.3 121.1	125.6 122.8 125.8	138.4 130.4 136.0	163.3 143.6 148.9	147.2 138.3 140.6	130.2 129.4 129.8	123.2 128.7 129.3	127.7 [c] 129.2	122.5 128.7 129.3	162.8 129.4 129.8	
2a	153.8 156.2	117.2 121.7	125.6 [c]	138.0 130.0	164.6 151.1	147.1 141.3	134.5 136.9	[c] 128.9	124.9 122.4	122.2 128.9	162.1 136.9	
2b	153.7 156.1	117.0 121.3	125.5 125.9	137.9 136.9	164.7 150.9	144.6 140.1	135.4 129.8	[c] [c]	138.5 138.6	122.1 [c]	162.2 129.8	21.5 22.3
3a	148.9	118.4	121.7	142.7	165.4	147.7	124.2	137.1	130.4	122.3	165.1	
3b	148.8	118.1	121.3	143.6	165.5	145.3	125.2	137.0	139.8	122.1	165.2	22.5
4a	148.8 146.6 184.4	118.0 120.9 148.9	125.2 125.1 143.7	137.1 136.3 130.0	164.1 148.5 129.9	147.4 139.4 [c]	131.6 123.9 132.0	122.7 125.7 131.2	124.5 [c] 129.8	122.5 141.6 128.9	162.6 166.0	
4b	148.7 146.6	117.8 120.5	125.2 125.1	137.1 136.2	164.2 145.0	144.2 139.8	137.0 124.3	122.7 124.9	125.1 [c]	122.4 142.6	162.7 166.1	21.5 23.0
	[c]	[c]	129.9	148.8	[c]	[c]	131.2	132.2	[c]			

[a] Shift assignments are based on correlations with free ligands, literature precedent and the accompanying compounds; the assignments are *tentative*. First row corresponds to {(2-aryl-κC^2)pyridine-κN} ligand as shown in illustration; second row corresponds to remaining 2-aryl-pyridine (**1a**, **2a**, **b**) or pyridyl fragment (**4a**, **b**); third row corresponds to other 2-phenyl-pyridine (**1a**) or diphenylacetylene fragment (**4a**, **b**).

[b] Limited solubility of **1b** prevented data acquisition.

[c] Obscured by solvent or unobserved.

Table 3
Crystallographic data for [bis(2-phenyl-pyridine)Ni{(2-phenyl-κC^2)pyridine-κN}]OTf (**1a**), [(2-phenyl-pyridine)BrNi{(2-phenyl-κC^2)pyridine-κN}] (**2a**), Ni{(2-phenyl-κC^2)pyridine-κN}$_2$ (**3a**), and [(2-phenyl-κC^2)pyridine-κN]Ni[2-(2-(1,2-diphenylethenyl-κC^2)phenyl)pyridine-κN] (**4a**)

	1a	**2a**	**3a**	**4a**
Formula	$C_{34}H_{26}N_3O_3F_3SNi$[a]	$C_{22}H_{17}BrN_2Ni$	$C_{22}H_{16}N_2Ni$	$C_{36}H_{26}N_2Ni$
Formula weight	1499.92[a]	520.11[e]	444.69[f]	545.32
Space group	$P\bar{1}$	$P\bar{1}$	$C2/c$	$P2_1/c$
Z	2[a]	2	8	4
a (Å)	15.0530(9)	10.001(3)	24.2023(8)	10.6170(5)
b (Å)	15.1416(10)	10.593(4)	11.7116(4)	16.0815(6)
c (Å)	15.6322(10)	11.718(4)	14.5953(4)	15.6065(6)
α (°)	95.366(2)	81.212(18)	90	90
β (°)	102.954(2)	71.227(18)	92.563(1)	96.212(2)
γ (°)	93.317(3)	84.383(18)	90	90
V (Å^3)	3445.7(4)	1160.0(7)	4132.9(2)	2648.97(19)
r_{calc} (g cm^{-3})	1.446	1.489	1.431	1.367
μ (mm^{-1})	0.684	2.579	0.959	0.761
Temperature (K)	173(2)	173(2)	173(2)	173(2)
λ (Å)	0.71073	0.71073	0.71073	0.71073
R indices $[I > 2\sigma(I)]$[b,c]	$R_1 = 0.0431$	$R_1 = 0.0266$	$R_1 = 0.0326$	$R_1 = 0.0333$
	$wR_2 = 0.1196$	$wR_2 = 0.0679$	$wR_2 = 0.0842$	$wR_2 = 0.0877$
R indices (all data)[b,c]	$R_1 = 0.0703$	$R_1 = 0.0384$	$R_1 = 0.0429$	$R_1 = 0.0516$
	$wR_2 = 0.1307$	$wR_2 = 0.0708$	$wR_2 = 0.0896$	$wR_2 = 0.0952$
Goodness-of-fit[d]	1.054	1.066	1.041	1.061

[a] The asymmetric unit is twice the formula unit plus one free 2-phenyl-pyridine molecule; the formula weight refers to the asymmetric unit, as does Z.
[b] $R_1 = \sum||F_o| - |F_c||/\sum|F_o|$.
[c] $wR_2 = \left[\sum w(|F_o| - |F_c|)^2 / \sum wF_o^2\right]^{1/2}$.
[d] GOF (all data) $= [\sum w(|F_o| - |F_c|)^2/(n-p)]^{1/2}$, n = number of independent reflections, p = number of parameters.
[e] The asymmetric unit contains one formula unit and a molecule of THF, as does Z.
[f] The asymmetric unit contains one formula unit and 1/2 of a 2-phenyl-pyridine molecule, as does Z.

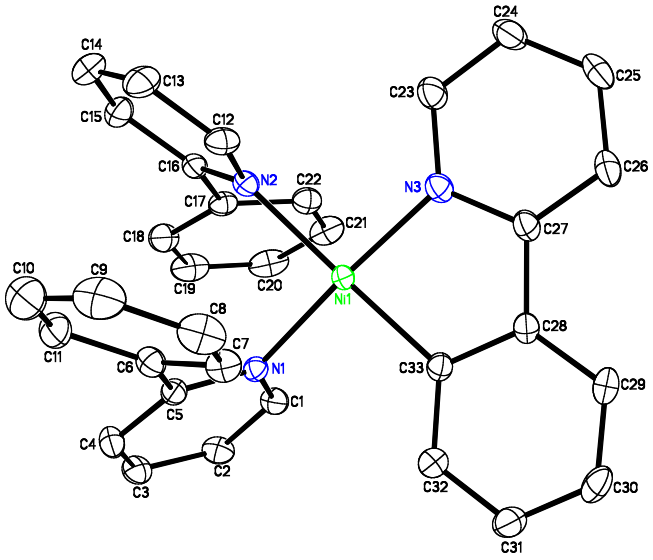

Fig. 1. Molecular view of one disorder model of the [bis(2-phenyl-pyridine)Ni{(2-phenyl-κC^2)pyridine-κN}] cation of the triflate salt **1a**.

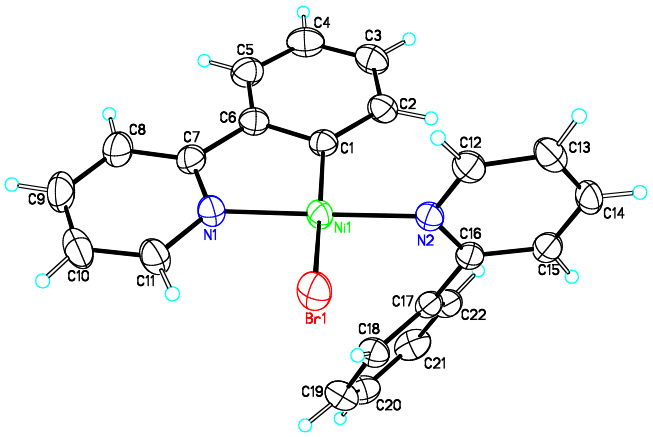

Fig. 2. Molecular view of (2-phenyl-pyridine)BrNi{(2-phenyl-κC^2)pyridine-κN} (**2a**).

position of Br$^-$ versus pyridine is somewhat nebulous, hence it is unknown whether **2a** and **2b** are the thermodynamic products.

2.1.4. Structure of (2-phenyl-pyridine)BrNi{(2-phenyl-κC^2)pyridine-κN}

A molecular view of (2-phenyl-pyridine)BrNi{(2-phenyl-κC^2)pyridine-κN} (**2a**) is given in Fig. 2, while the crystallographic details and core metric parameters are given in Tables 3 and 4, respectively. The bite angle of the cyclometalate is 84.62(7)°, and the accompanying Ni–κC and Ni–κN distances are 1.9044(18) and 1.9169(16) Å, respectively. The Ni–κN bond is shorter than in the other examples below, in part because it is opposite the relatively weak 2-phenyl-pyridine donor. There is a strain affiliated with the cyclometalate evidenced in internal versus external Ni–κC–C angles of 112.60(13)° and 130.09(14)°, and related Ni–κN–C angles of 115.25(12)° and 126.76(14)°, respectively. The (2-phenyl-κC^2)pyridine-κN ligand is

Table 4
Core distances (Å) and angles (°) for [(2-phenyl-pyridine)BrNi{(2-phenyl-κC^2)pyridine-κN}] (**2a**), Ni{(2-phenyl-κC^2)pyridine-κN}$_2$ (**3a**), and [(2-phenyl-κC^2)pyridine-κN]Ni[2-(2-(1,2-diphenylethenyl-κC^2)phenyl)pyridine-κN] (**4a**)

	2a	3a	4a
Ni–κC	1.9044(18)	1.887(2)	1.8911(10)
		1.892(2)	
Ni–κN	1.9169(16)	1.9794(16)	1.9556(9)
		1.9610(18)	
Ni–N(κN′)	1.9018(15)		1.9336(10)[a]
Ni–Br	2.4410(7)		
Ni–κC′			1.8844(10)[a]
C′=C			1.3462(15)[a]
κN–Ni–κC	84.62(7)	84.66(8)	84.78(4)
		84.73(8)	
Ni–κC–C	112.60(13)[b]	113.26(15)[b]	113.07(8)[b]
	130.09(14)[c]	130.23(16)[c]	130.94(8)[c]
		112.73(16)[b]	
		130.48(17)[c]	
Ni–κN–C	115.25(12)[b]	112.46(13)[b]	113.69(7)[b]
	126.76(14)[c]	126.99(15)[c]	127.87(9)[c]
		113.95(14)[b]	
		126.32(15)[c]	
κN–Ni–N	173.29(6)		
κC–Ni–N	90.01(7)		
κN–Ni–Br	96.24(5)		
κC–Ni–Br	167.32(5)		
N–Ni–Br	89.89(5)		
κN′–Ni–κC′			84.53(4)[e]
κN–Ni–κC′		156.24(8)[d]	175.41(4)[e]
		161.08(8)[d]	171.61(4)[e]
κN–Ni–κN′		101.27(7)[d]	97.42(4)[e]
κC–Ni–κC′		97.07(9)[d]	93.87(5)[e]
Ni–κC′–C(Ph)			115.81(8)[e]
Ni–κC′=C			119.79(8)[e]

[a] Prime refers to carbon of cyclometalate insertion ring.
[b] Internal cyclometalate angle.
[c] External cyclometalate angle.
[d] Angles defined with primes are between two different cyclometalates.
[e] Angles defined with primes are between the cyclometalate and the cyclometalate insertion ring (primed).

clearly ''pinched'' in binding to the first row metal. There is a slight rippling of the pseudo square planar molecule, as the κN–Ni–N angle is 173.29(6)° and the κC–Ni–Br angle is 167.32(5)°. Two of the remaining core angles (κC–Ni–N = 90.01(7)° and N–Ni–Br = 89.89(5)°) are regular such that the Br–Ni–κC–N plane is flat. The Ni–Br distance is normal (92.4410(7) Å) as is the remaining Ni–N(py) distance of 1.9018(15) Å.

2.1.5. Alkylation attempts

The generation of alkyl derivatives was sought as a means to investigate the potential of this ligand framework with regard to olefin oligomerization [20]. Unfortunately, repeated attempts to alkylate the slightly more soluble tolyl bromide derivative, (2-tolyl-pyridine)BrNi{(2-tolyl-κC^2)pyridine-κN} (**2b**), were unsuccessful. In certain runs utilizing MeLi or Me_2Zn, a red material, possessing a new aromatic signature and a singlet in a region (δ 0.52) potentially indicative of metalation, was observed in <10% yield by ^{1}H NMR spectroscopy. Along with black material presumed to be Ni^0, GC–MS confirmed the presence of 2-(2,4-xylyl)-pyridine and 2-tolyl-pyridine in a rough 1:2 ratio. The products implicate reductive elimination from (2-tolyl-pyridine)MeNi{(2-tolyl-κC^2)pyridine-κN} as potential degradation path [21].

2.2. Double cyclometalation

2.2.1. Synthesis of Ni{(2-aryl-κC^2)pyridine-κN}$_2$

While attempting to synthesize a neutral cyclometalation species through the addition of R$^-$ and X$^-$, KO^{t}Bu was utilized in Et_2O, and the aforementioned red color again appeared. With this reagent, the red, crystalline double cyclometalation product, Ni{(2-phenyl-κC^2)pyridine-κN}$_2$ (**3a**), was produced from its corresponding cation, [bis(2-phenyl-pyridine)Ni{(2-phenyl-κC^2)pyridine-κN}]OTf (**1a**) [16,22]. Difficulties in separating 2-phenyl-pyridine from the product limited isolation procedures to slow crystallizations, and yields exceeding 40% were sometimes produced; most were substantially lower. In addition to the aforementioned alkyl anion equivalents, amide bases were also tried with limited success. These problems prompted a change in synthetic procedures, and the bromides (2-phenyl-pyridine)BrNi{(2-phenyl-κC^2)pyridine-κN} (**2a**) and (2-tolyl-pyridine)BrNi{(2-tolyl-κC^2)pyridine-κN} (**2b**) were subjected to KO^{t}Bu in Et_2O to afford Ni{(2-aryl-κC^2)pyridine-κN}$_2$ (aryl = phenyl, **3a**; tolyl, **3b**) in modest, but reproducible yields (>30%). The two cyclometalated ligands appear equivalent in ^{1}H and ^{13}C{^{1}H} NMR spectra, consistent with a 2-fold symmetry axis, but two structural isomers were deemed plausible, prompting an X-ray structural study.

2.2.2. Structure of Ni{(2-phenyl-κC^2)pyridine-κN}$_2$

Structural details are listed in Table 3 and core features of Ni{(2-phenyl-κC^2)pyridine-κN}$_2$ (**3a**) are listed in Table 4. Fig. 3 illustrates the rippled geometry of **3a**, whose two cyclometalates possess bite angles of 84.66(8)° and 84.73(8)°. The pinched geometry of this unit is also observed in the aforementioned internal versus external Ni–κC–C and Ni–κN–C angles to the same degree as in **2a**. In this derivative, the *d*(Ni–κN) of 1.9794(16) and 1.9610(18) Å are substantially longer than in **2a**, perhaps reflecting the strong *trans*-influence of the opposing nickel–carbon bonds, while the *d*(Ni–κC) are essentially the same at 1.887(2) and 1.892(2) Å. Accompanying the longer Ni–κN is a wider κN–Ni–κN angle of 101.27(7)° in comparison to the κC–Ni–κC angle of 97.07(9)°. The distortion from square planar results in intermetalate κC–Ni–κN′ angles of 161.08(8)° and 156.24(8)°, and a dihedral angle between cyclometalate κC–Ni–κN planes of 31.9°. The structurally characterized Pt analogue has very similar metric parameters aside from chelate bite angles of 79.3°, which are a consequence of longer Pt–C (1.984, 2.002 Å) and Pt–N (2.125, 2.128 Å) bonds, and accompanying κC–Ni-κN′ angles of 176.4° and 176.8°. The latter renders

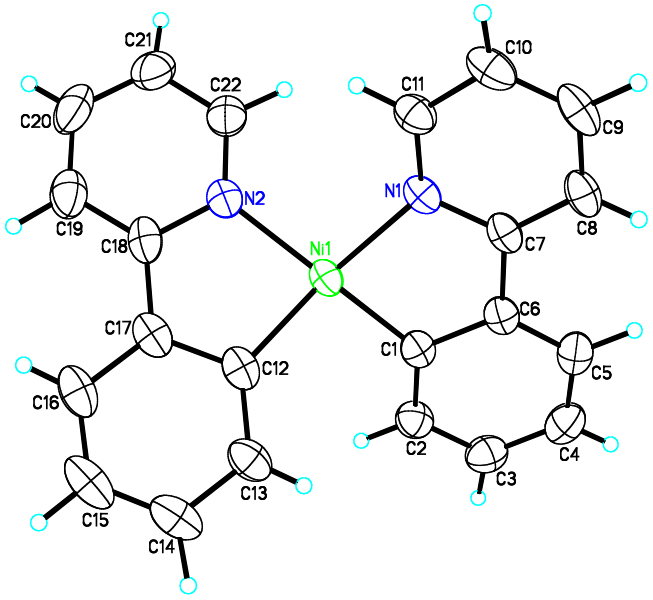

Fig. 3. Molecular view of Ni{(2-phenyl-κC^2)pyridine-κN}$_2$ (**3a**).

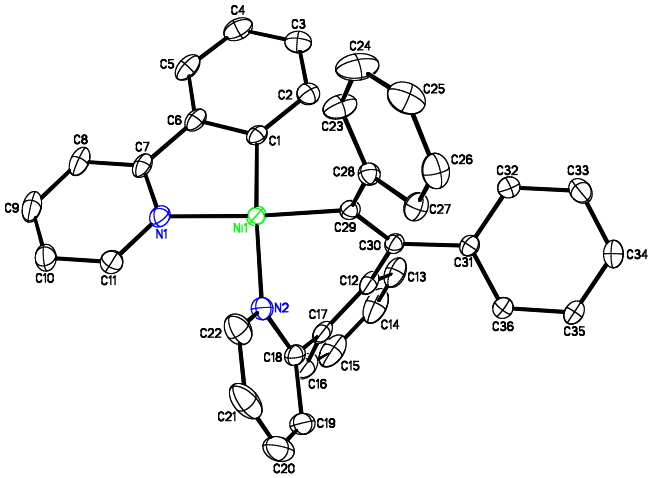

Fig. 4. Molecular view of [(2-phenyl-κC^2)pyridine-κN]Ni[2-(2-(1,2- diphenylethenyl-κC^2)phenyl)pyridine-κN] (**4a**).

the aforementioned dihedral angle to be only 4.0°, hence the Pt derivative is relatively flat [23].

2.2.3. Diphenylacetylene insertion

The stronger field imparted by the Ni–carbon bonds in this system may be offset by the less than perfect bite angle of the cyclometalated ligand. In an attempt to generate five-coordinate species more accommodating to the bite angle of the (2-phenyl-κC^2)pyridine-κN ligand, Ni{(2-aryl-κC^2)pyridine-κN}$_2$ (aryl = phenyl, **3a**; tolyl, **3b**) were treated with diphenylacetylene in the hopes of making an adduct. Instead, the PhCCPh group inserted into the carbon arm of one of the cyclometalates [24,25], generating [(2-aryl-κC^2)pyridine-κN]Ni[2-(2-(1,2-diphenylethenyl-κC^2)aryl)pyridine-κN] (aryl = phenyl, **4a**; *p*-tolyl, **4b**) according to Scheme 1. The seven-membered ring of insertion product **4a** may have more than one conformer; over time, solutions of **4a** form an equilibrium mixture with another minor species (**4a′**) possessing related spectral features. No further evaluation of this process was conducted.

2.2.4. Structure of [(2-phenyl-κC^2)pyridine-κN]Ni[2-(2-(1,2-diphenylethenyl-κC^2)phenyl)pyridine-κN]

Fig. 4 illustrates a molecular view of [(2-phenyl-κC^2)pyridine-κN]Ni[2-(2-(1,2-diphenylethenyl-κC^2)phenyl)pyridine-κN] (**4a**), and crystallographic details can be found in Table 3, while selected metric parameters are given in Table 4. The geometry of the (2-phenyl-κC^2)pyridine-κN ligand is similar to **3a**, with *d*(Ni–κC) and *d*(Ni–κN) of 1.8911(10) and 1.9556(9) Å, respectively, and a bite angle of 84.78(8)° along with the usual distortions. The pyridine and its accompanying phenyl ring are greatly twisted relative to each other, as are the phenyls of the Ph_2C_2 fragment, and the buckling of the seven-membered ring (primed) enables the pseudo square planar molecule to be only modestly distorted: ∠κN′–Ni–κC′ = 84.53(4)°, ∠κN–Ni–κN′ = 97.42(4)°, ∠κC–Ni–κC′ = 93.87(4)°, and ∠κN–Ni–κC′ = 175.41(4)°, 171.61(4)°. The remaining angles and distances of the ring-expanded fragment are fairly normal, with *d*(Ni–κC′) = 1.8844(10)° and *d*(Ni–κN′) = 1.9336(10)°.

3. Discussion

3.1. Heterolytic CH-bond activation

As according to precedent, the 2-aryl-pyridine ligands were found to undergo heterolytic CH-bond activation, but the exact details of the process remain uncertain. Scheme 2 illustrates some mechanistic possibilities [26]. Alkylation of (2-tolyl-pyridine)BrNi{(2-tolyl-κC^2)pyridine-κN} (**2b**) provided hints of an intermediate Ni–Me complex, but this species did *not* generate Ni{(2-tolyl-κC^2)pyridine-κN}$_2$ (**3b**) via the loss of MeH; instead, evidence of reductive elimination and degradation was found. The addition of *tert*-butoxide to (2-phenyl-pyridine)BrNi{(2-phenyl-κC^2)pyridine-κN} (**2a**) and (2-tolyl-pyridine)BrNi{(2-tolyl-κC^2)pyridine-κN} (**2b**) did generate the bis-cyclometalates, Ni{(2-aryl-κC^2)pyridine-κN}$_2$ (aryl = phenyl, **3a**; tolyl, **3b**), but the path to product is unclear. It is conceivable that a Ni–O^{t}Bu species forms and it is electrophilic enough to enable an abstraction, or perhaps dissociation of ^{t}BuO$^-$ is necessary. In this instance, an exogenous ^{t}BuO$^-$ would deprotonate a cationic intermediate coordinated by an *ortho*-CH-bond of the aryl group. In an attempt to isolate this intermediate as a B(C$_6$H$_3$-3,5-(CF$_3$)$_2$)$_4$ salt, H[BAr$^F_4$] was added to Ni{(2-tolyl-κC^2)pyridine-κN}$_2$ (**3b**) [27], but the reagent merely induced a disproportion to produce [bis(2-tolyl-pyridine)Ni{(2-tolyl-κC^2)pyridine-κN}][BAr$^F_4$] (**1b′**). This reaction was confirmed by stoichiometry studies: 3/2 **3b** + 2H[BAr$^F_4$] → **1b′** + 1/2[Ni(II)][BAr$^F_4$]$_2$. Loss of ^{t}BuO$^-$ may occur to a greater extent than R$^-$ or NR$_2^-$,

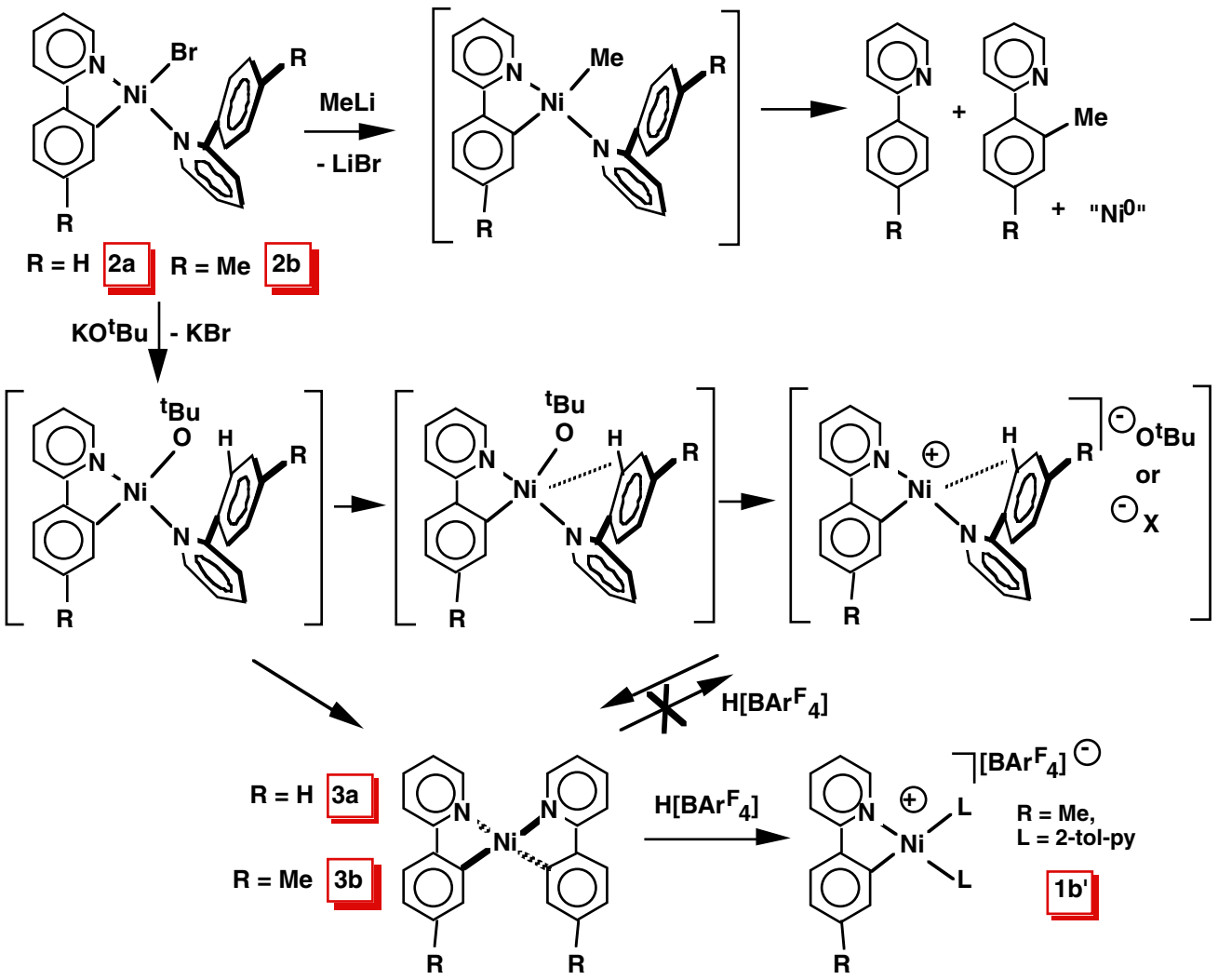

Scheme 2.

perhaps favoring the dissociative mechanism. It may simply be the competition between a non-productive reductive elimination path, and an internal abstraction/deprotonation that favors the *tert*-butoxide as the effective base for the second cyclometalation.

3.2. Nature of the bonding in Ni{(2-aryl-κC^2)pyridine-κN}$_2$

This study purported to take advantage of the strong fields imparted by metal–aryl bonds, and the low spin, diamagnetic character of the compounds containing the (2-aryl-κC^2)pyridine-κN certainly provides supporting evidence. In addition, a standard DFT calculation was conducted on Ni{(2-phenyl-κC^2)pyridine-κN}$_2$ (**3a**) and according to the d-orbital splitting diagram in Fig. 5, a rather strong field is indeed present. While the actual energies provided by the calculation appear overestimated, they represent a large splitting between the sigma-antibonding $d_{x^2-y^2}$ orbital and the essentially non-bonding set of d_{z^2}, d_{yz}, d_{xy} and d_{xz} orbitals. A rough assumption of square planar geometry ($10\,Dq \sim E(d_{x^2-y^2}) - E(d_{xy})$) affords a $10\,Dq$ of $>40\,000\ cm^{-1}$, which is well above fields supported solely by more electronegative donors (i.e., halides, O- and N-based ligands) [28]. Despite the rippled geometry that would tend to attenuate the antibonding character of d_{z^2}, this orbital is still the HOMO in the system. In order to determine the preference for the *trans*-κC–κN configuration of the cyclometalates in **3a**, one of these ligands was "flipped" to give an *trans*-κN–κN, *trans*-κC–κC geometry, and geometry optimization gave a structure with very similar metric parameters. This arrangement was found to be ~3 kcal/mol above the true geometry, lending credence to the strong *trans*-influence of the nickel–aryl bonds, even though the distortion renders these interactions well away from 180° (156° and 161°).

4. Experimental

4.1. General considerations

All manipulations were performed using either glovebox or high-vacuum techniques. Hydrocarbon and ethereal sol-

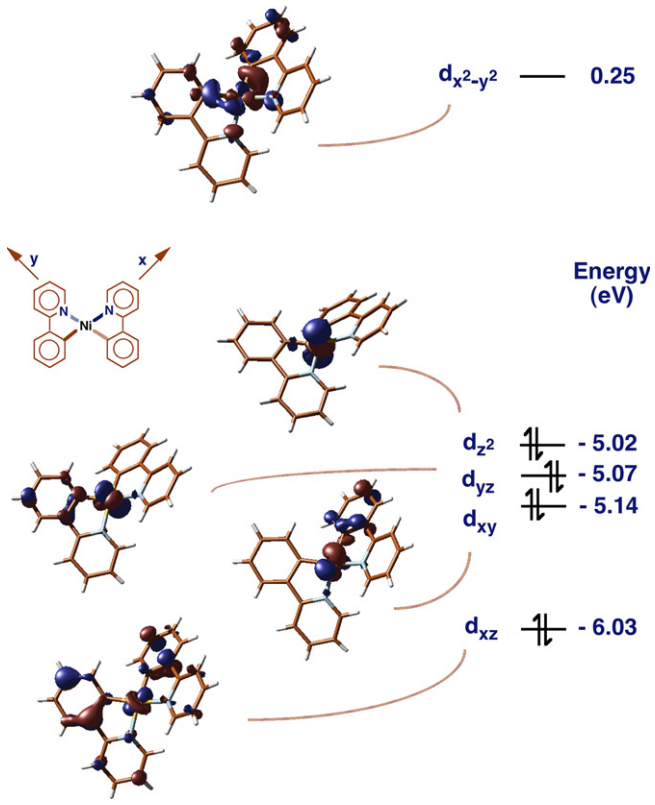

Fig. 5. d-Orbital splitting diagram for Ni{(2-phenyl-κC^2)pyridine-κN}$_2$ (**3a**).

vents were dried over and vacuum transferred from sodium benzophenone ketyl (3-4 ml tetraglyme/L was added to hydrocarbons). Benzene-d_6 was sequentially dried over sodium and stored over sodium or 4 Å molecular sieves. All glassware was base-washed and oven dried. Nickel(II)triflate was prepared according to literature procedures [19]. Diphenylacetylene (Aldrich) was used as received; 2-phenyl-pyridine and 2-*p*-tolyl-pyridine (Aldrich) were degassed and stored under nitrogen; KBr (Mallinckrodt) and LiBr (Aldrich) were dried for 4 days in a 150 °C oven and stored under nitrogen. KO^{t}Bu (Alfa Aesar) was sublimed and stored under nitrogen.

^{1}H- and ^{13}C{^{1}H}-NMR spectra were obtained using Mercury-300, Inova-400, and Inova-500 spectrometers. Combustion analyses were performed by Robertson Microlit Laboratories, Madison, NJ.

4.2. Procedures

4.2.1. [Bis(2-aryl-pyridine)Ni{(2-aryl-κC^2)pyridine-κN}]OTf (aryl = phenyl, **1a**; tolyl, **1b**; OTf = trifluoromethansulfonate)

A neat mixture of nickel(II)triflate (10.0 g, 28.0 mmol) and 2-phenyl-pyridine (20.0 g, 118 mmol) was heated at 180 °C in a bomb reaction vessel for 18 h. The resulting dark brown oil was triturated with THF (60 ml), giving a brown solution with yellow solid. This mixture was filtered and washed with THF (3 × 20 ml) to yield 8.5 g of yellow solid (43%). Recrystallization of **1a** from hot toluene resulted in formation of bright yellow crystals suitable for X-ray diffraction. The same procedure was followed for **1b**, yielding a yellow-green solid (45%).

4.2.2. (2-Aryl-pyridine)BrNi{(2-aryl-κC^2)pyridine-κN} (aryl = phenyl, **2a**; tolyl, **2b**)

To a mixture of **1a** (1.49 mmol) and KBr (2.00 g, 16.8 mmol) was distilled 20 ml THF at −78 °C. A dark orange color developed as the solution was warmed to 23 °C and stirred for 10 min. After stirring for 6 h, the amber solution was filtered, the salt cake washed several times with THF, and the filtrate reduced in volume to 5 ml. Ether (15 ml) was added and the mixture was stirred for 10 min at 23 °C, yielding 400 mg (60%) of bright orange solid (**2a**) which was collected by filtration. The same procedure was followed for **2b** except that LiBr was used in place of KBr. A red-orange solid was isolated in 62% yield. Anal. Calc. for $H_{21}C_{24}BrN_2Ni$ (**4b**): C, 60.55; H, 4.45; N, 5.88. Found: C, 60.33; H, 4.73; N, 5.59%.

4.2.3. Ni{(2-aryl-κC^2)pyridine-κN}$_2$ (aryl = phenyl, **3a**; tolyl, **3b**)

To a 250 ml flask charged with placed **2a** (2.00 g, 5.45 mmol) and KO^{t}Bu (612 mg, 5.45 mmol) and attached to a swivel frit was distilled 100 ml ether at −78 °C. The solution was allowed to warm to 23 °C and stirred for 3 h. Upon warming, the solution attained a dark red color. The resulting solution was filtered through the frit, the solid washed five times with ether, and the red solution concentrated to 10 ml and cooled to −78 °C. This was filtered cold to leave a red solid (536 mg, 32%). X-ray diffraction quality crystals were obtained by cooling a concentrated solution of the solid in ether to −35 °C. The same procedure was followed for **3b** with **2b** as the starting material (34%). Anal. Calc. for $H_{20}C_{24}N_2Ni$ (**2b**): C, 72.95; H, 5.10; N, 7.09. Found: C, 70.55; H, 4.84; N, 6.80%.

4.2.4. [(2-Aryl-κC^2)pyridine-κN]Ni[2-(2-(1,2-diphenylethenyl- κC^2)aryl)pyridine-κN] (aryl = phenyl, **4a**; tolyl, **4b**)

To a bomb reaction vessel of **3a** (70.0 mg, 0.191 mmol) and diphenylacetylene (34.0 mg, 0.191 mmol) was distilled 10 ml benzene at −78 °C. The vessel was allowed to warm to 23 °C and then placed in a 35 °C oil bath. This was slowly heated to 100 °C and remained at this temperature for 8 h. The resulting dark solution was stripped of solvent, triturated with ether, and filtered to give 54 mg of orange-brown solid (52% yield). Covering a solution of **4a** in toluene with hexanes yielded orange-red, X-ray diffraction quality crystals. Leaving **4a** in benzene solution led to the appearance of a new product by ^{1}H NMR, proposed to be a conformational isomer (**4a**′). K_{eq}(**4a** → **4a**′) = 0.43. ^{1}H NMR (benzene-d_6): δ 9.05 (d, 1H, J = 6.0), 8.51 (d, 1H, J = 5.0), 8.06 (d, 1H, J = 5.5), 7.58 (d, 1H, J = 7.5), 7.51 (m, 1H), 7.28–6.75 (m, 17H), 6.52 (d, 2H, J = 5.5),

6.34 (“t,” 1H, $J = 6.0$), 6.19 (“t,” 1H, $J = 6.0$). The same procedure was followed for **4b**, which was isolated as an orange-brown solid (50%).

4.3. Calculation details

All calculations were done using the GAUSSIAN 03 program [29]. Computations were performed at the B3PW91 level of theory, employing Becke's three-parameter hybrid DFT/HF exchange functional [30] and Perdew and Wang's non-local exchange parameter [31]. The CEP-31G effective core potential basis set was used [32–34]. Atomic coordinates from the X-ray structure of **3a** were used, and in all cases geometry optimizations were carried out without symmetry constraints.

Acknowledgements

P.T.W. thank the National Science Foundation (CHE-0415506) and Cornell University for financial support. The DFT study was done as an assignment for Chem 665 under the direction of Prof. Barry K. Carpenter.

Appendix A. Supplementary material

CCDC 645421, 645423, 645422 and 645424 contain the supplementary crystallographic data for **1a**, **2a**, **3a** and **4a**. These data can be obtained free of charge via http://www.ccdc.cam.ac.uk/conts/retrieving.html, or from the Cambridge Crystallographic Data Centre, 12 Union Road, Cambridge CB2 1EZ, UK, fax: (+44) 1223-336-033, or e-mail: deposit@ccdc.cam.ac.uk. Supplementary data associated with this article can be found, in the online version, at doi:10.1016/j.jorganchem.2007.06.047.

References

[1] P.J. King, Organomet. Chem. 30 (2002) 282.
[2] (a) Y. Jean, F. Volatron, J. Burdett, An Introduction to Molecular Orbitals, Oxford Univ. Press, New York, 1993;
(b) T.A. Albright, J.K. Burdett, Problems in Molecular Orbital Theory, Oxford Univ. Press, New York, 1992.
[3] A.D. Ryabov, Chem. Rev. 105 (2005) 503.
[4] J. Dupont, C.S. Consorti, J. Spencer, Chem. Rev. 105 (2005) 2527.
[5] W. Henderson, Adv. Organomet. Chem. 54 (2006) 207.
[6] R.H. Crabtree, The Organometallic Chemistry of the Transition Metals, fourth ed., John Wiley & Sons, New York, 2005.
[7] J.P. Collman, L.S. Hegedus, J.R. Norton, R.G. Finke, Principles and Applications of Organotransition Metal Chemistry, University Science Books, Mill Valley, CA, 1987.
[8] A. Kasahara, Bull. Chem. Soc. Jpn. 41 (1968) 1272.
[9] B.N. Cockburn, D.V. Howe, T. Keating, B.F.G. Johnson, J. Lewis, J. Chem. Soc., Dalton Trans. 4 (1973) 404.
[10] M.I. Bruce, B.L. Goodall, I. Matsuda, Aust. J. Chem. 28 (1975) 1259.
[11] (a) S. Sprouse, K.A. King, P.J. Spellane, R.J. Watts, J. Am. Chem. Soc. 106 (1984) 6647;
(b) K. Dedelan, P.I. Djurovich, F.O. Garces, G. Carlson, R.J. Watts, Inorg. Chem. 30 (1991) 1685.
[12] V. Grushin, N. Herron, D.D. LeCloux, W.J. Marshall, V.A. Petrov, Y. Wang, J. Chem. Soc., Chem. Commun. (2001) 1494.
[13] (a) S. Lamansky, P. Djurovich, D. Murphy, F. Razzaq-Abdel, H.-E. Lee, C. Adachi C, P.E. Burrows, S.R. Forrest, M.E. Thompson, J. Am. Chem. Soc. 123 (2001) 4304;
(b) A. Tamayo, B. Alleyne, P.I. Djurovich, I.T. Lamansky, N. Ho, R. Bau, M.E. Thompson, J. Am. Chem. Soc. 125 (2003) 7377.
[14] R.L. Lagadec, L. Alexandrova, H. Estevez, M. Pfeffer, V. Laurinavičius, J. Razumiene, A.D. Ryabov, Eur. J. Inorg. Chem. 14 (2006) 2735.
[15] D. Kalyani, N.R. Deprez, L.V. Desai, M.S. Sanford, J. Am. Chem. Soc. 127 (2005) 7330, This paper describes C–H activation of 2-phenylpyridine derivatives by Pd(II), followed by C–C bond formation to form a variety of *ortho*-arylated products.
[16] A.R. Dick, J.W. Kampf, M.S. Sanford, J. Am. Chem. Soc. 127 (2005) 12790.
[17] K.L. Hull, W.Q. Anani, M.S. Sanford, J. Am. Chem. Soc. 128 (2006) 7134, C–H activation of quinoline and 2-phenylpyridine derivatives by Pd(II), followed by fluorination resulted in a variety of *ortho*-fluorinated compounds.
[18] K.L. Hull, E.L. Lanni, M.S. Sanford, J. Am. Chem. Soc. 128 (2006) 14047, The Pd(II)/(IV) cycle is employed in the oxidative coupling of several 2-phenylpyridine derivatives, resulting in a variety of functionalized biaryls.
[19] Y. Inada, Y. Nakano, M. Inamo, M. Nomura, S. Funahashi, Inorg. Chem. 39 (2000) 4793.
[20] (a) T.R. Younkin, E.F. Connor, J.I. Henderson, S.K. Friedrich, R.H. Grubbs, D.A. Bansleben, Science 287 (2000) 460;
(b) E.F. Connor, T.R. Younkin, J.I. Henderson, A.W. Waltman, R.H. Grubbs, Chem. Commun. (2003) 2272;
(c) A.W. Waltman, T.R. Younkin, R.H. Grubbs, Organometallics 23 (2004) 5121.
[21] K. Tamao, J. Organometal. Chem. 653 (2002) 23.
[22] M. Sanford has produced the compound from 2 equiv of 2-(2-lithiophenyl)-pyridine and a Ni(II) source; personal communication.
[23] (a) For a structure of the Pt analogue, see: L. Chassot, E. Müller, A. von Zelewsky, Inorg. Chem. 23 (1984) 4249;
(b) , The Pd analogue has also been synthesized. See:P. Jolliet, M. Gianini, A. von Zelewsky, G. Bernardinelli, H. Stoeckli-Evans, Inorg. Chem. 35 (1996) 4883.
[24] J.M. Huggins, R.G. Bergman, J. Am. Chem. Soc. 103 (1981) 3002.
[25] M.A. Bennett, S.A. Macgregor, E. Wenger, Helv. Chim. Acta 84 (2001) 3084.
[26] M. Lersch, M. Tilset, Chem. Rev. 105 (2005) 2471.
[27] A. Toner, J. Matthes, S. Gründemann, E. Clot, H.-H. Limbach, B. Donnadieu, S. Sabo-Etienne, B. Chaudret, J. Am. Chem. Soc. 122 (2000) 6777.
[28] B.N. Figgis, M.A. Hitchman, Ligand Field Theory and Its Applications, Wiley-VCH, New York, 2000.
[29] M.J. Frisch, G.W. Trucks, H.B. Schlegel, G.E. Scuseria, M.A. Robb, J.R. Cheeseman, J.A. Montgomery Jr., T. Vreven, K.N. Kudin, J.C. Burant, J.M. Millam, S.S. Iyengar, J. Tomasi, V. Barone, B. Mennucci, M. Cossi, G. Scalmani, N. Rega, G.A. Petersson, H. Nakatsuji, M. Hada, M. Ehara, K. Toyota, R. Fukuda, J. Hasegawa, M. Ishida, T. Nakajima, Y. Honda, O. Kitao, H. Nakai, M. Klene, X. Li, J.E. Knox, H.P. Hratchian, J.B. Cross, C. Adamo, J. Jaramillo, R. Gomperts, R.E. Stratmann, O. Yazyev, A.J. Austin, R. Cammi, C. Pomelli, J.W. Ochterski, P.Y. Ayala, K. Morokuma, G.A. Voth, P. Salvador, J.J. Dannenberg, V.G. Zakrzewski, S. Dapprich, A.D. Daniels, M.C. Strain, O. Farkas, D.K. Malick, A. D Rabuck, K. Raghavachari, J.B. Foresman, J.V. Ortiz, Q. Cui, A.G. Baboul, S. Clifford, J. Cioslowski, B.B. Stefanov, G. Liu, A. Liashenko, P. Piskorz, I. Komaromi, R.L. Martin, D.J. Fox, T. Keith, M.A. Al-Laham, C.Y. Peng, A. Nanayakkara, M. Challacombe, P.M.W. Gill, B. Johnson, W. Chen, M.W. Wong, C. Gonzalez, J.A. Pople, GAUSSIAN 03, Revision C.02, Gaussian, Inc., Wallingford CT, 2004.

[30] J.M. Becke, J. Chem. Phys. 98 (1993) 5648.
[31] J.P. Perdew et al., Phys. Rev. B 46 (1992) 6671.
[32] W.J. Stevens, H. Basch, M. Krauss, J. Chem. Phys. 81 (1984) 6026.
[33] W.J. Stevens, M. Krauss, H. Basch, P.G. Jasien, Can. J. Chem. 70 (1992) 612.
[34] T.R. Cundari, W.J. Stevens, J. Chem. Phys. 98 (1993) 5555.